

## The *Bacillus subtilis* Signaling Protein SpoIVB Defines a New Family of Serine Peptidases

Ngo T. Hoa,<sup>1</sup> James A. Brannigan,<sup>2</sup> and Simon M. Cutting<sup>1\*</sup>

School of Biological Sciences, Royal Holloway University of London, Egham, Surrey, TW20 0EX,<sup>1</sup> and Department of Chemistry, University of York, York, YO10 5DD,<sup>2</sup> United Kingdom

Received 19 July 2001/Accepted 8 October 2001

**The protein SpoIVB plays a key role in signaling in the  $\sigma^K$  checkpoint of *Bacillus subtilis*. This regulatory mechanism coordinates late gene expression during development in this organism and we have recently shown SpoIVB to be a serine peptidase. SpoIVB signals by transiting a membrane, undergoing self-cleavage, and then by an unknown mechanism activating a zinc metalloprotease, SpoIVFB, which cleaves pro- $\sigma^K$  to its active form,  $\sigma^K$ , in the outer mother cell chamber of the developing cell. In this work we have characterized the serine peptidase domain of SpoIVB. Alignment of SpoIVB with homologues from other spore formers has allowed site-specific mutagenesis of all potential active site residues within the peptidase domain. We have defined the putative catalytic domain of the SpoIVB serine peptidase as a 160-amino-acid residue segment at the carboxyl terminus of the protein. His236 and Ser378 are the most important residues for proteolysis, with Asp363 being the most probable third member of the catalytic triad. In addition, we have shown that mutations at residues Asn290 and His394 lead to delayed signaling in the  $\sigma^K$  checkpoint. The active site residues suggest that SpoIVB and its homologues from other spore formers are members of a new family of serine peptidases of the trypsin superfamily.**

The protein SpoIVB has recently been identified as a serine peptidase that plays a central role in a regulatory checkpoint (the  $\sigma^K$  checkpoint) which coordinates gene expression during the later stages of spore formation in *Bacillus subtilis* (36). Proteolytic activity has been demonstrated in vitro as well as in vivo and this activity is essential to SpoIVB's role as the signaling molecule that activates  $\sigma^K$ .

SpoIVB is synthesized in the forespore chamber of the sporulating cell and is secreted across the inner forespore membrane. At this point SpoIVB becomes proteolytically active and self-cleaves into at least three distinct species, of 46, 45, and 44 kDa. These are thought to be the active forms which signal proteolytic processing of the transcription factor  $\sigma^K$ . Signaling leads to activation of a processing complex embedded in the outer forespore membrane which cleaves the N-terminal leader sequence (the pro sequence) from pro- $\sigma^K$ . The sigma factor  $\sigma^K$  is then competent to direct the final stages of gene expression in the mother cell. Reminiscent of the blood clotting cascades, SpoIVB is also subject to secondary proteolysis, which presumably inactivates SpoIVB by cleaving the active species into 42- and 40-kDa forms (36). How SpoIVB activates processing of pro- $\sigma^K$  is not yet clear, but genetic evidence has shown that SpoIVB most likely interacts with one or more members of the pro- $\sigma^K$  processing complex which is embedded in the outer forespore membrane (7, 8, 10). These proteins are SpoIVFB, a zinc metalloprotease which cleaves pro- $\sigma^K$  (10, 28), and the BofA and SpoIVFA proteins, both of which are required to inhibit activity of SpoIVFB (25, 26). Interestingly, both SpoIVFA and BofA inhibit SpoIVFB using

their C termini, which are exposed to the space between the inner and outer forespore membranes, and removal of either the BofA or SpoIVFA C terminus renders SpoIVFB constitutively active (12, 27, 34).

SpoIVB also carries a PDZ domain in the N-terminal half of the polypeptide (21). PDZ domains are used by signaling molecules for protein targeting and protein-protein interactions (18, 21, 22). In other work we have shown that this SpoIVB PDZ domain could be involved in multiple interactions including oligomerization, interaction with an inhibitor protein, BofC, and activating processing of pro- $\sigma^K$  (14). The bacterial Prc (also called Tsp) and HtrA (also called DegP) serine peptidase families carry both a PDZ and peptidase domain (19, 21) and it has been shown that substrate recognition is mediated by the PDZ domain (3). An attractive model for how SpoIVB signals is that SpoIVB uses its PDZ domain to target one or both of the SpoIVFB inhibitors (SpoIVFA and BofA) followed by cleavage of the C termini of these inhibitors. An alternative role for the serine peptidase activity is simply to enable secretion of SpoIVB across the inner forespore membrane since SpoIVB does not carry a normal N-terminal signal sequence.

Homologues of SpoIVB proteins have been identified in a number of spore-forming organisms, revealing a string of strictly conserved residues. In this work we have examined the serine peptidase domain of SpoIVB with the aim of defining amino acid residues involved in catalysis. It appears that SpoIVB is a distinctive variant of trypsin-like proteases and that PDZ domains commonly have a specialized role in bacteria for the activation and substrate recognition of proteases that have to cross a membrane.

### MATERIALS AND METHODS

**Bacterial strains.** Strains used in this work are listed in Table 1 and were all congeneric with the prototrophic *spo*<sup>+</sup> strain PY79. To construct lysogens of

\* Corresponding author. Mailing address: School of Biological Sciences, Royal Holloway University of London, Egham, Surrey, TW20 0EX, United Kingdom. Phone: 44-(0)1784-443760. Fax: 44-(0)1784-434326. E-mail: s.cutting@rhul.ac.uk.

TABLE 1. *B. subtilis* strains

Strain	Genotype	Construction or reference <sup>a</sup>
Established strains		
PY79	<i>spo</i> <sup>+</sup>	38
SC433	<i>SPβ::gerE-lacZ</i>	9
SC1836	<i>spoIVBΔ::spc</i>	17
NH578	<i>spoIVBΔ::spc amyE::spoIVB</i> <sup>+</sup>	pNH470 into SC1836
NH577	<i>spoIVBΔ::spc amyE::pDG364</i>	pDG364 into SC1836
Nonconservative mutants		
NH1377	<i>spoIVBΔ::spc amyE::spoIVBDL213</i>	pNH1375 into SC1836
NH1320	<i>spoIVBΔ::spc amyE::spoIVBH236</i>	pNH1308 into SC1836
NH1345	<i>spoIVBΔ::spc amyE::spoIVBDL240</i>	pNH1342 into SC1836
NH1346	<i>spoIVBΔ::spc amyE::spoIVBDL242</i>	pNH1343 into SC1836
NH1347	<i>spoIVBΔ::spc amyE::spoIVBNI290</i>	pNH1344 into SC1836
NH1380	<i>spoIVBΔ::spc amyE::spoIVBKA321</i>	pNH1376 into SC1836
NH1326	<i>spoIVBΔ::spc amyE::spoIVBDL363</i>	pNH1314 into SC1836
NH1328	<i>spoIVBΔ::spc amyE::spoIVBSK378</i>	pNH1316 into SC1836
NH1455	<i>spoIVBΔ::spc amyE::spoIVBKA378</i>	pNH1445 into SC1836
NH1330	<i>spoIVBΔ::spc amyE::spoIVBHD394</i>	pNH1318 into SC1836
Conservative mutants		
NH1451	<i>spoIVBΔ::spc amyE::spoIVBHF236</i>	pNH1441 into SC1836
NH1452	<i>spoIVBΔ::spc amyE::spoIVBDN242</i>	pNH1442 into SC1836
NH1453	<i>spoIVBΔ::spc amyE::spoIVBDN363</i>	pNH1443 into SC1836
NH1454	<i>spoIVBΔ::spc amyE::spoIVBSA378</i>	pNH1444 into SC1836

<sup>a</sup> Mutations were created in pBluescript clones carrying the *spoIVB* gene, sequenced, and subcloned into pDG364 to give the plasmid clones indicated. These subclones were then linearized and DNA was introduced into the *amyE* locus of SC1836 cells as described in Materials and Methods.

*SPβ::gerE-lacZ* a phage lysate was prepared from strain SC433 and used for transduction of appropriate recipient strains. For integration of DNA at the *amyE* locus, cells were transformed with linearized DNA (11). Strain constructions using DNA-mediated transformation are outlined briefly in Table 1.

**General methods.** General *Bacillus* methods (transduction, transformation, antibiotic selection, etc.) were performed as described by Cutting and Vander-Horn (11). Sporulation methods, including the induction of sporulation by the resuspension method, resistance measurements, and assays of *gerE*-directed β-galactosidase synthesis, were performed as described previously (16).

**Site-specific mutagenesis.** Two oligonucleotide primers were used to amplify by PCR a 1,429-bp *spoIVB* product using chromosomal DNA from *B. subtilis* strain PY79 as a template. The primers were P1 (5'-TTATAACGTTTCGTGCA CATCCATTCGTTTC-3'), annealing to nucleotides -146 to -127 from the *spoIVB* start codon, and P2 (5'-AACGGATCCAGTCAGCTTGCTTTTCTTTTCC-3'), which annealed to the *spoIVB* stop codon (bold) and a further 18 bases downstream. The PCR product contained *Hind*III (P1) and *Bam*HI (P2) restriction sites (underlined), enabling direct cloning into pBluescript II KS(+). The resultant clone, pNH252, was sequenced completely to verify the presence of an unmodified *spoIVB* cistron. Next, mutations were created with mismatched oligonucleotides using the method of Kunkel as described in Sambrook et al. (29). pBluescript clones were verified by the presence of a single base change by DNA sequencing. Finally, the *spoIVB* genes were subcloned as 1.4-kb *Hind*III-*Bam*HI fragments into pDG364 (11) and are listed in Table 1. pDG364 enables the insertion of cloned DNA, in *trans*, at the *amyE* locus by a double-crossover marker replacement. In each case we linearized the pDG364 subclones by digestion with *Xho*I and introduced them into SC1836 (*spoIVBΔ::spc*) cells by DNA-mediated transformation followed by selection for chloramphenicol resistance (Cm<sup>r</sup>; encoded by pDG364). Insertion at the *amyE* locus was confirmed by testing for an Amy<sup>-</sup> phenotype (failure to digest starch) as described elsewhere (11). We also constructed two isogenic control strains, NH578 (*spoIVBΔ::spc amyE::spoIVB*<sup>+</sup>) and NH577 (*spoIVBΔ::spc amyE::pDG364*). NH578 was created by integrating a pDG364 subclone, pNH470, carrying the full-length, 1,429-bp, wild-type *spoIVB* gene into the *amyE* locus and NH577 was created by integrating the unmodified pDG364 plasmid into the chromosome by a double-crossover recombination event at *amyE*.

**Western blotting analysis.** Samples (1 ml) were taken from sporulating cultures and cells were harvested by centrifugation and frozen in liquid N<sub>2</sub>. To break cells, pellets were suspended in 50 μl of TS buffer (25 mM Tris-HCl [pH 7.4], 0.1 M NaCl) containing lysozyme (0.2 μg/ml) and incubated for 10 min on ice. Fifty microliters of 2× sodium dodecyl sulfate-polyacrylamide gel electrophoresis

(SDS-PAGE) loading dye was then added and the samples were sonicated for 10 s before gel loading (approximately 20 μl of sample/well). Immunoblotting of sporulating extracts with polyclonal antiserum to SpoIVB was performed as described previously (12, 36).

**Expression of SpoIVB templates in *Escherichia coli*.** A pET28b clone (pΔIVB) containing a truncated SpoIVB template starting at codon 37 of *spoIVB* and fused to the ribosome binding site and ATG start codon of the pET vector has been described (36). Identical clones were made carrying mutant *spoIVB* templates *spoIVBH236* (pΔIVBH236), *spoIVBDL242* (pΔIVBDL242), *spoIVBDL363* (pΔIVBDL363), and *spoIVBSK378* (pΔIVBSK378).

## RESULTS

**Site-directed mutagenesis of putative peptidase catalytic residues.** Figure 1 shows a sequence alignment of the C-terminal domains (residues 188 to 425 in *B. subtilis* SpoIVB) of SpoIVB homologues from four *Bacillus* species (*B. subtilis*, *B. anthracis*, *B. stearothermophilus*, and *B. halodurans*), two *Clostridium* species (*C. acetobutylicum* and *C. difficile*), and *Carboxythermus hydrogenoformans*. This region lies downstream of the PDZ domain (residues 102 to 186 in *B. subtilis* SpoIVB). The availability of sequences from such divergent sources aids the definition of strictly conserved residues. A single serine (Ser378) is conserved among these proteins. Proteolysis in vivo and in vitro is inhibited by the serine peptidase inhibitor diisopropylfluorophosphate and a mutation at this serine (SA378) inhibits autoproteolysis of SpoIVB (36). In addition, residues (GMSG) flanking this serine are conserved and are reminiscent of the SA clan of serine peptidases, which comprise the trypsin superfamily (1, 23) which has recently been reclassified as clan PA(S) (24). As has been discussed previously, this is the most likely candidate for the active site serine (36). The catalytic domain of most (but not all) serine peptidases consists of a triad of three residues (histidine, aspartic acid, and serine), with their order and spacing defining the clan and family of the



FIG. 1. Protein sequence alignment of SpoIVB peptidase domains. Sequences were aligned using ClustalW (32) and the figure was generated using ALSCRIPT (2). Abbreviations: Bsub, *B. subtilis* (accession no. P17896, residues 187 to 425); Bhal, *B. halodurans* (Q9K975, 197 to 437); Cdif, *C. difficile* (Q46028, 124 to 352); Bant, *B. anthracis* (www.tigr.org/tdb/mdb/mdbinprogress.html); Chyd, *C. hydrogenoformans* (www.tigr.org/tdb/mdb/mdbinprogress.html); Bste, *B. steartothermophilus* (www.genome.ou/bstearo.html); Cace, *C. acetobutylicum* (www.genomecorp.com/genesequences/clostridium/clospage.html). Sequences without accession numbers were derived from the unfinished genome DNA sequences. Strictly conserved amino acids are boxed, positions of the SpoIVB mutants described are labeled and numbered, and the putative catalytic triad residues are highlighted with an asterisk.

peptidase (23). Clans indicate a common evolutionary origin, usually assigned following determination of three-dimensional structure, while families are primarily defined by sequence homology. The alignment reveals four conserved Asp residues (positions 213, 240, 242, and 363) that could form the acidic part of the catalytic triad. Only two His residues (positions 326 and 394) are conserved which could represent the base that enhances the nucleophilicity of the active site serine. Conserved lysine residues (positions 321 and 387) were also targeted for mutagenesis as they could potentially perform the role of a base. Examples include  $\beta$ -lactamase and Tsp, which have a catalytic Ser-Lys dyad (1). Similarly, the conserved asparagine at position 290 was mutated, since Asn residues are known to be involved in oxyanion stabilization in some proteases (e.g., subtilisin) or are important in orienting catalytic His residues in cysteine proteases. A number of conservative and more drastic, nonconservative replacements were introduced into the sites predicted to be important in catalytic activity (Table 2).

**In vivo effects of SpoIVB mutations.** All mutations were created in a pBluescript *spoIVB* clone, which carried the entire *spoIVB* gene. The mutated *spoIVB* clone was sequenced to verify the presence of a single base change and then subcloned into the plasmid pDG364. When linearized, this plasmid enables cloned DNA to be introduced at the *amyE* locus by a double-crossover recombination event (11). The mutant *spoIVB* alleles were incorporated at *amyE* in cells carrying a null mutation at the *spoIVB* locus, *spoIVBΔ::spc*. Using isogenic control strains with (NH578) or without (NH577) a copy of the wild-type *spoIVB* gene at *amyE* we examined sporulation and signaling.

As shown in Table 2 there were three distinct classes of mutant phenotype. The first group (group I) consisted of *spoIVBHN236*, *spoIVBHF236*, *spoIVBDL242*, *spoIVBDL363*, *spoIVBSA378*, and *spoIVBSK378* mutants which caused a severe effect on spore formation, with the failure to produce heat- or lysozyme-resistant spores. Spore formation was arrested at stage III-IV with the production of limited numbers of phase-grey spores. This phenotype was essentially asporogenous and indistinguishable from the null *spoIVBΔ::spc* mutant. The pDG364 plasmids carrying these mutant alleles were introduced into *spo*<sup>+</sup> cells (strain PY79) and in each case we found that the resulting phenotype was Spo<sup>+</sup>, showing that the mutation was recessive to the wild-type *spoIVB* gene when placed at its normal chromosomal position (data not shown).

The second phenotypic class (group II) was made up of strains carrying the *spoIVBDL213*, *spoIVBDL240*, *spoIVBDN242*, *spoIVBKA321*, *spoIVBDN363*, and *spoIVBKA387* alleles. Cells carrying these mutations produced normal levels of heat- and lysozyme-resistant spores and were essentially indistinguishable from the isogenic Spo<sup>+</sup> strain, NH578. Spores produced in these mutants were able to germinate normally.

The final and most interesting mutant class (group III) comprised the *spoIVBNI290* and *spoIVBHD394* mutations. They formed phase-bright spores, and so were Spo<sup>+</sup>, but there was a marked and reproducible reduction in the level of spores produced (approximately 30% fewer spores than in the wild-type strain). For these mutants we examined the capacity of spores to germinate and found that they were germination defective. Further analysis revealed that for *spoIVBNI290* this germination defect was temperature sensitive, since the mutant was unable to germinate properly at 37°C. In other work

TABLE 2. *spoIVB* alleles

Strain <sup>a</sup>	Relevant allele	Mutation <sup>b</sup>	Heat resistance <sup>c</sup>	Lysozyme resistance <sup>c</sup>	Germination phenotype <sup>d</sup>	Signaling <sup>e</sup>
NH577	<i>spoIVBΔ::spc</i>	Insertion-deletion	$4.9 \times 10^{-5}$	$1.56 \times 10^{-2}$	ND	–
NH578	<i>spoIVB</i> <sup>+</sup>	Wild type	88	54.4	+	+
NH1377	<i>spoIVBDL213</i>	Asp213 to Leu	98	94.5	+	+
NH1320	<i>spoIVBHN236</i>	His236 to Asn	$1.18 \times 10^{-4}$	$1.12 \times 10^{-2}$	ND	–
NH1451	<i>spoIVBHF236</i>	His236 to Phe	$2.3 \times 10^{-4}$	$6.9 \times 10^{-3}$	ND	–
NH1345	<i>spoIVBDL240</i>	Asp240 to Leu	95.7	55.7	+	+
NH1346	<i>spoIVBDL242</i>	Asp242 to Leu	$1.12 \times 10^{-3}$	$2.19 \times 10^{-2}$	ND	–
NH1452	<i>spoIVBDN242</i>	Asp242 to Asn	87.6	45	+	+
NH1347	<i>spoIVBNI290</i>	Asn290 to Ile	28.9	29	+	(30°C), – (37°C)
NH1380	<i>spoIVBKA321</i>	Lys321 to Ala	86	88	+	+
NH1326	<i>spoIVBDL363</i>	Asp363 to Leu	$1.54 \times 10^{-4}$	$3.7 \times 10^{-2}$	ND	–
NH1453	<i>spoIVBDN363</i>	Asp363 to Asn	77.6	42	+	+
NH1328	<i>spoIVBSK378</i>	Ser378 to Lys	$1.76 \times 10^{-4}$	$1.77 \times 10^{-2}$	ND	–
NH1454	<i>spoIVBSA378</i>	Ser378 to Ala	$3.25 \times 10^{-4}$	$3.26 \times 10^{-3}$	ND	–
NH1455	<i>spoIVBKA387</i>	Lys387 to Ala	68.1	57	+	+
NH1330	<i>spoIVBHD394</i>	His394 to Asp	26.7	34.7	– (30°C), – (37°C)	Delayed

<sup>a</sup> See Table 1.

<sup>b</sup> See Fig. 1.

<sup>c</sup> Heat or lysozyme resistance of cultures 24 h after the initiation of sporulation in DS medium (16). Values are expressed as percentages of CFU per milliliter in the untreated culture.

<sup>d</sup> Five-day-old colonies grown on sporulation agar were tested for their capacity to germinate normally on tetrazolium agar plates as described previously (16). All strains that were phenotypically Spo<sup>–</sup> were not tested for a germination phenotype (ND).

<sup>e</sup> Signaling was defined according to the following two criteria: firstly, formation of pigmented colonies (Pig<sup>+</sup>) associated with the production of the  $\sigma^K$ -expressed CotA protein (30), and secondly, expression of the  $\sigma^K$ -controlled reporter gene, *gerE-lacZ*, in cells containing an *SPβgerE-lacZ* lysogen (see Fig. 2) as described previously (9).

we have shown that *bofA* and *bofB* mutations (in BofA and SpoIVFA, respectively) allow constitutive activation of SpoIVFB and therefore pro- $\sigma^K$  processing (8). This, in turn, leads to premature  $\sigma^K$ -controlled gene expression, a reduction in spore-forming efficiency, and for those spores that are formed (approximately 10% of the total CFU), a defective germination response. This phenotype is most probably caused by a defect in spore coat assembly, which is controlled by the  $\sigma^K$  regulon. We reasoned that the reduced sporulation effi-

ciency and defective germination response of the NI290 and HD394 mutants could be caused by a defect in signaling.

**$\sigma^K$ -directed gene expression.** To examine signaling in the  $\sigma^K$  checkpoint we used a  $\sigma^K$ -transcribed reporter gene, *gerE-lacZ* (9). Lysogenized cells carrying mutant alleles with the *SPβgerE-lacZ* reporter phage were examined for *gerE*-directed  $\beta$ -galactosidase synthesis during spore formation (Fig. 2). For the *spoIVB* null mutant (SC1836 *spoIVBΔ::spc*) we detected low levels (less than 15%) of  $\sigma^K$ -directed gene expression, in

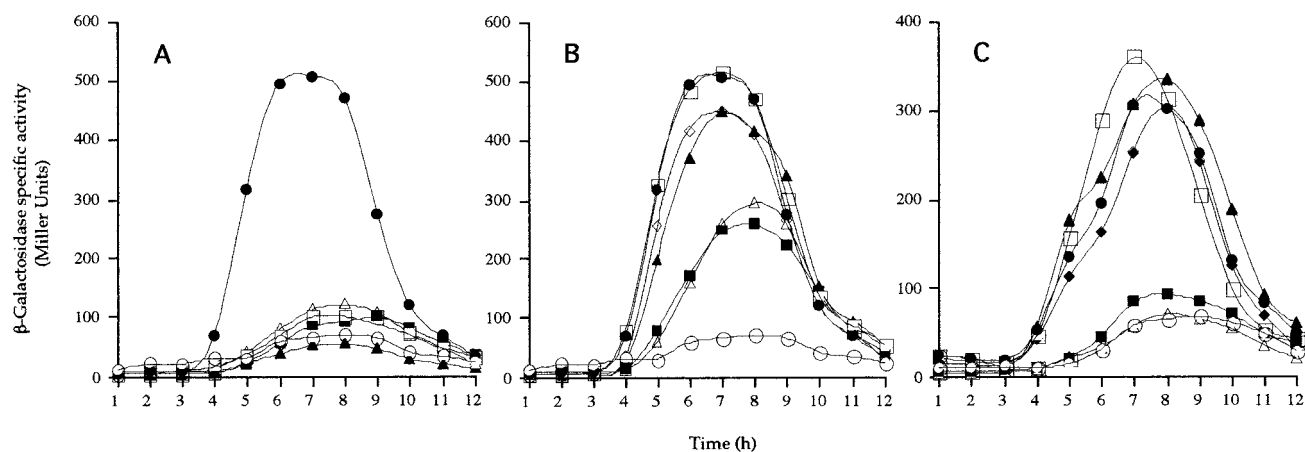


FIG. 2. *gerE-lacZ* expression in *spoIVB* mutants.  $\beta$ -Galactosidase synthesis was measured at the indicated times following the initiation of sporulation in cells carrying the *SPβgerE::lacZ* reporter phage. In each case congenic strains were used and the relevant alleles (at the *amyE* locus) are given here (see Table 1 for complete genotypes). (A) ●, NH578, *spoIVB*<sup>+</sup>; ○, NH577, *spoIVBΔ::spc*; △, NH1326, *spoIVBDL363*; ▲, NH1328, *spoIVBSK378*; □, NH1320, *spoIVBHN236*; ■, NH1346, *spoIVBDL242*. (B) ●, NH578, *spoIVB*<sup>+</sup>; ○, NH577, *spoIVBΔ::spc*; □, NH1345, *spoIVBDL240*; ■, NH1347, *spoIVBNI290*; △, NH1330, *spoIVBHD394*; ▲, NH1377, *spoIVBDL213*; ◇, NH1380, *spoIVBKA321*. (C) ●, NH578, *spoIVB*<sup>+</sup>; ○, NH577, *spoIVBΔ::spc*; ■, NH1451, *spoIVBHF236*; □, NH1452, *spoIVBDN242*; ▲, NH1453, *spoIVBDN363*; △, NH1454, *spoIVBSA378*; ◆, NH1455, *spoIVBKA387*.



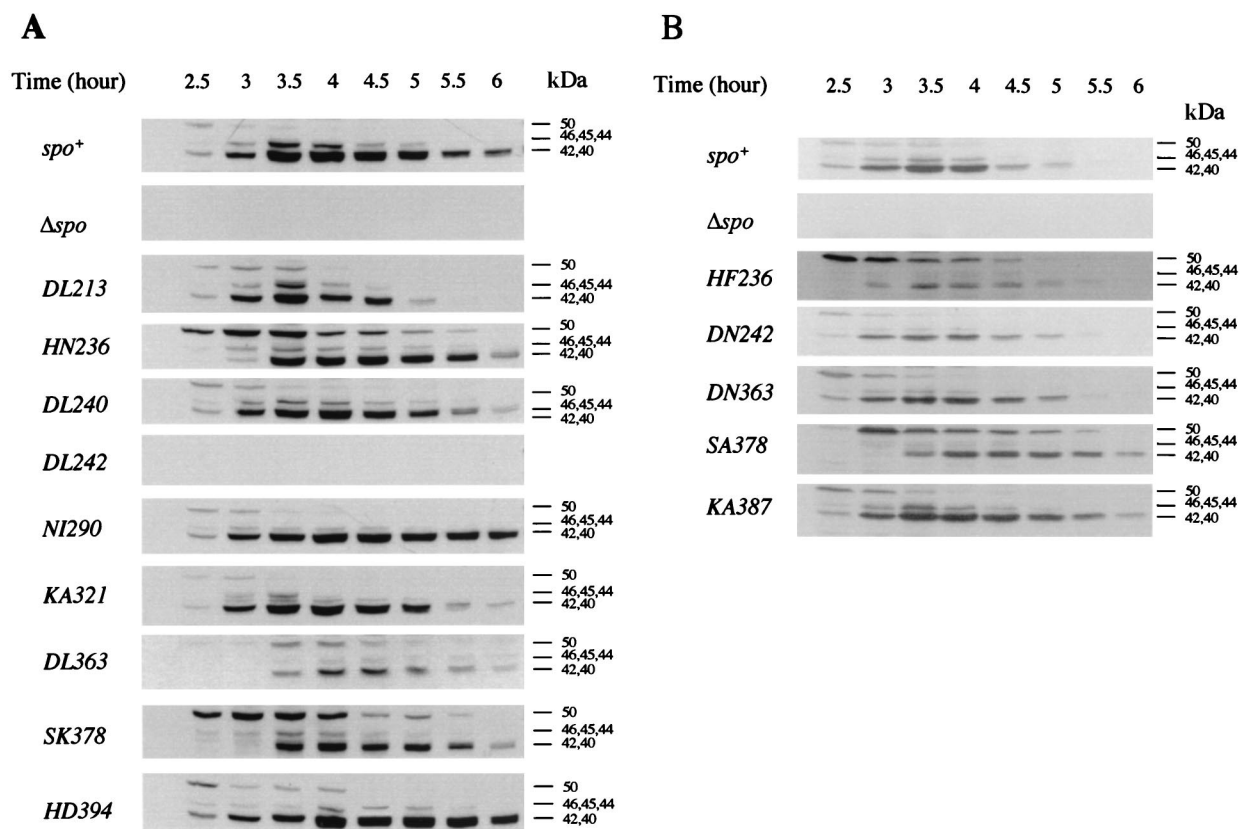


FIG. 3. Proteolysis of SpoIVB in *B. subtilis*. Sporulation was induced in wild-type (*spo*<sup>+</sup>), *spoIVB* $\Delta::spc$  ( $\Delta spo$ ), and *spoIVB* mutant strains. Panel A shows an experiment examining strains carrying nonconservative mutations, and panel B shows strains carrying conservative changes as well as the alteration KA378. Samples of sporulating cells were taken at the times indicated, cells were lysed, and equivalent amounts of cellular protein were fractionated by SDS-PAGE (12%) and examined with a polyclonal antiserum to SpoIVB (2-min enhanced chemiluminescence exposure time). The full-length, 50-kDa, unprocessed form of SpoIVB is marked, as are 46-, 45-, and 44-kDa intermediate SpoIVB cleavage products and the 42- and 40-kDa cleavage products produced by secondary cleavage.

agreement with previous work, while for *spo*<sup>+</sup> cells, *gerE-lacZ* expression started at about 3.5 to 4 h after the initiation of spore formation. Our results define three clear classes of mutant gene expression, with (i) a block in  $\sigma^K$ -directed gene expression, (ii) no effect on  $\sigma^K$ -directed gene expression, and (iii) delayed and reduced levels of expression. These mutant phenotypes correspond exactly to the groups classified above according to their ability to sporulate.

The group I mutant strains with a null sporulation phenotype have essentially abolished or severely reduced *gerE-lacZ* expression (Fig. 2A and C). The second group comprised the mutants with no detectable sporulation defect. These strains expressed *gerE-lacZ* at the same time and at the same levels as in *spo*<sup>+</sup> cells (Fig. 2B and C). The third group caused a clear delay (1 h) and reduction in the level of *gerE-lacZ* expression (Fig. 2B). As mentioned above, defective signaling can lead to defects in spore coat assembly and spore germination. Here, gene expression was delayed, in contrast to mutations in *bofA* and *bofB* that allow constitutive processing of pro- $\sigma^K$ , leading to premature  $\sigma^K$ -directed gene expression. Although other alleles within *spoIVB* have been shown to lead to delayed signaling (14, 17), the clear delay seen in the *spoIVBH394* and *spoIVBNI290* mutations reinforces the notion that the role of this checkpoint is as a timing mechanism. That signaling

does occur accounts for the levels of phase-bright spores that are produced.

**Proteolysis of SpoIVB.** To determine the effect of our collection of mutations on proteolysis we examined SpoIVB during spore formation using a polyclonal antiserum (Fig. 3). Previous work has shown that SpoIVB is synthesized as a 50-kDa polypeptide at about the second hour of sporulation (36). Starting at hour 3, SpoIVB is cleaved into a number of products (approximately 46, 45, and 44 kDa), one or more of which is the active form that signals SpoIVFB-mediated processing of pro- $\sigma^K$ . Almost simultaneously, these forms are subject to secondary proteolysis, which presumably inactivates the active forms by cleavage to 42- and 40-kDa species which are then cleaved further. During sporulation, then, in wild-type cells, we see the 50-kDa species briefly but at hour 3 autoproteolysis has begun producing the active species as well as the inactive forms.

The effects on SpoIVB proteolysis are shown in Fig. 3. It must be stressed that these Western blots are particularly difficult to interpret due to the appearance of intermediate species in the blots and our accuracy in sampling. Regardless, we have repeated these blots at least twice and are confident of the following classifications by residue.

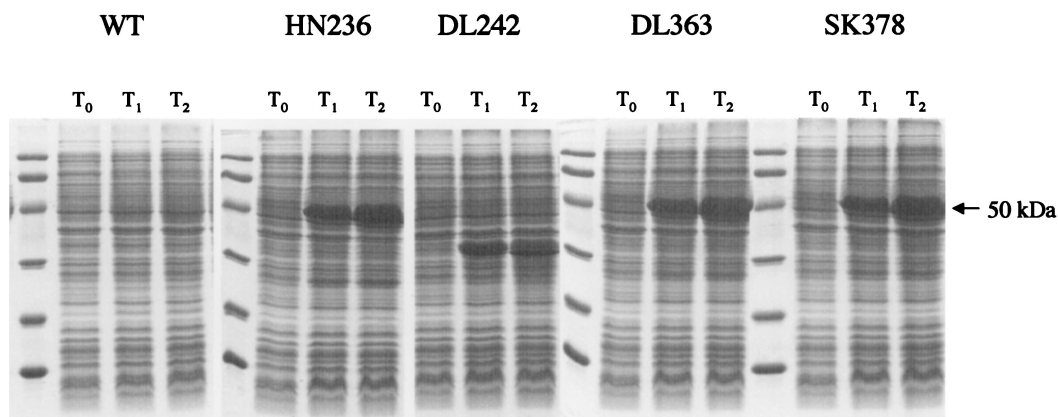


FIG. 4. Expression of mutant SpoIVB proteins in *E. coli*. *E. coli* BL21 (DE3) cells harboring pET28b vectors with a wild-type (WT) SpoIVB or mutant genes (*spoIVBHN236*, *spoIVBDL242*, *spoIVBDL363*, and *spoIVBSK378*) were grown and gene expression was induced with isopropyl- $\beta$ -D-thiogalactopyranoside (IPTG). Samples taken before induction ( $T_0$ ) and at hours 1 ( $T_1$ ) and 2 ( $T_2$ ) postinduction were fractionated by SDS-PAGE (12.5%). The full-length 50-kDa SpoIVB precursor protein is indicated by an arrow.

(i) **His236 and Ser378.** Compared to *spo*<sup>+</sup> cells, in HN236 (Fig. 3A), HF236 (Fig. 3B), SK378 (Fig. 3A), and SA378 (Fig. 3B) mutants, the 50-kDa SpoIVB protein was cleaved less quickly and appeared to be maintained longer in its full-length form. Compared to *spo*<sup>+</sup> cells the 50-kDa species appeared to undergo proteolysis approximately 30 min later as judged by the appearance of the 40- to 42-kDa species. This corresponds to hour 3 using our sampling regimen shown in Fig. 3. We must emphasize that differences in actual processing time compared to previous studies (36) are empirical and must be taken in the context of processing relative to that in *spo*<sup>+</sup> cells. With some mutants such as KA387 (Fig. 3B) and DL213 (Fig. 3A) there appeared to be slightly more of the 50-kDa species than with *spo*<sup>+</sup> cells at the same time points. However, processing initiated at the same time as in *spo*<sup>+</sup> cells (2.5 h). To confirm that proteolysis was defective in these mutant proteins, we expressed the HN236 and SK378 SpoIVB mutants from pET28b expression vectors in *E. coli* BL21(DE3) and examined expressed proteins by SDS-PAGE. As shown in Fig. 4, expression led to the accumulation of a stable, full-length 50-kDa SpoIVB species. In contrast, expression of a wild-type SpoIVB template produced little or no detectable SpoIVB protein as it is subject to rapid self-cleavage in *E. coli* (36).

(ii) **Asp213 (Fig. 3A), Asp240 (Fig. 3A), Lys321 (Fig. 3A), and Lys387 (Fig. 3B).** Processing in these mutants appeared to be normal in terms of the onset of proteolysis and clearance of the 50-kDa species. Our interpretation is also based on the ability of these mutants to signal processing of pro- $\sigma^K$  normally.

(iii) **Asp242.** We are unable to detect any SpoIVB DL242 mutant protein in *B. subtilis* (Fig. 3A). We have repeated this experiment a number of times and conclude that this mutant protein is unstable and presumably is rapidly cleared by secondary proteolysis. We confirmed this, in part, by expressing the SpoIVB DL242 protein in *E. coli* (Fig. 4), which showed that the mutant protein behaves differently from the wild-type protein, accumulating as a 35- to 40-kDa species. The aberrant molecular mass of this SpoIVB DL242 species implies that self-cleavage is defective and/or the protein is unstable. The latter deduction could arise if the structure of the mutant

polypeptide is abnormal. This corresponds with our results showing that signaling is defective in *spoIVBDL242* cells. In contrast, a conservative amino acid substitution at this position (Asp242 to Asn) allows normal signaling in the  $\sigma^K$  checkpoint, and proteolysis of the SpoIVB DN242 protein appears normal.

(iv) **Asn290 (Fig. 3A) and His394 (Fig. 3A).** Processing of these SpoIVB mutant proteins appeared essentially normal, although there was perhaps a slight accumulation of the 50-kDa species in *spoIVBHD394* cells. Although signaling is delayed in *spoIVBNI290* and *spoIVBHD394* mutants, we assume that the subtle change or delay in SpoIVB processing is not detectable by the 30-min sampling regimen used here.

(v) **Asp363.** Proteolysis appeared to be delayed by 30 min in *spoIVBDL363* mutant cells (Fig. 3A). Also, there appeared to be considerably less SpoIVB protein detectable by Western blotting. Expression of SpoIVB DL363 in *E. coli* showed a clear accumulation of a full-length 50-kDa precursor, showing that processing was defective. In contrast, processing in the mutant with a conservative replacement (SpoIVB DN363) was normal (Fig. 3B), as was signaling of pro- $\sigma^K$  processing.

## DISCUSSION

Our analysis of potential catalytic residues that comprise the serine peptidase domain has provided strong evidence for His236 and Ser378 as components of the active site, since substitution at these positions prevents signaling of pro- $\sigma^K$  processing as well as inhibiting the proteolytic activity of SpoIVB. As mentioned below it must be stressed that proteases can retain residual activity even when active site residues are altered (20). The order and spacing of His236 and Ser378 agree with serine peptidases of the trypsin superfamily (1, 23) and make the essential catalytic unit approximately 160 amino acid residues contained at the C terminus of SpoIVB. The GMSG motif surrounding Ser378 closely resembles trypsin, but it is a distinct variant as this family typically has a residue with negative charge (Asp or Glu) preceding the active site serine (1, 23). In contrast, there is little similarity in sequence around the active site SpoIVB His236 residue with

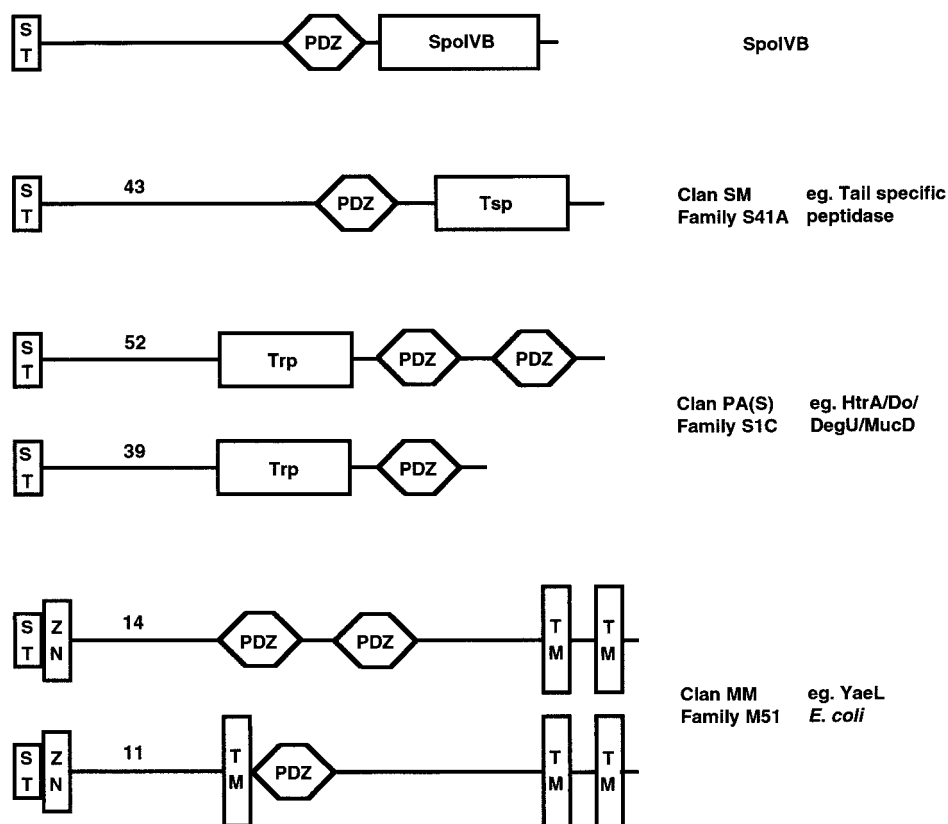


FIG. 5. Bacterial proteases with PDZ domains. Bacterial PDZ-containing proteins detected by the simple modular architecture research tool (SMART) (31) that are associated with peptidase activity are represented schematically with the number of proteins (as of June 2001) of each type indicated. Non-SpoIVB proteins are classified into three groups characterized by trypsin modules (Trp), carboxyl-terminal processing peptidases (Tsp), or zinc metallopeptidases (Zn). For simplicity, ST represents either a signal or transit peptide or a membrane-spanning segment. Also, only the transmembrane segments (TM) that are accurately predicted by SMART are represented for ease of comparison.

other trypsin family members, suggesting that SpoIVB must be a member of a new family of the PA(S) clan.

We have identified one Asp residue, Asp363, for which mutation to Leu leads to a lack of SpoIVB self-cleavage and signaling properties. Another Asp residue, Asp242, when mutated to Leu also blocked signaling yet failed to accumulate any protein at all, suggesting that the mutation rendered the protein unstable. We have noticed a DxxLL motif which is present in a number of serine peptidase families, especially those of the PA(S) clan (23, 24), and is found at position 363, and we take this as evidence that the SpoIVB serine peptidase has a catalytic triad with Asp363 as its third member. Intriguingly, a conservative change at this position does not disrupt proteolysis of the SpoIVB protein. The acidic residue is the least important component of the active site triad in serine peptidases, and Asp is replaced by Glu in carboxyl peptidase (37) and aspartyl dipeptidase (13). In the case of cytomegalovirus protease, histidine acts as the acid in a unique Ser-His-His triad. Mutation of cytomegalovirus protease His157 reduces activity only 5- to 10-fold (33). In contrast, catalysis by trypsin-like enzymes is severely impaired when the acidic residue is replaced by mutation, suggesting that the negative charge of the Asp side chain balances the positive charge that develops on the histidine during catalysis (6). In some systems, however,

the Asp simply serves to maintain the correct position of the active site histidine. Indeed, in cysteine proteases, a conserved Asn residue (e.g., Asn175 in papain) serves this very purpose (35) and Asn156 appears in the hydrolase catalytic triad of *E. coli* outer membrane phospholipase A (15). We assume that the role of Asp363 is to stabilize the appropriate His263 rotamer or tautomer in SpoIVB catalysis, a function that could potentially be performed by Asn. The unusually close spacing of Asp363 to Ser378, its ability to be replaced by Asn, and the lack of a consensus motif around His236 all argue that SpoIVB represents a new family of serine peptidases.

One observation we have made here is that mutations that block signaling of pro- $\sigma^K$  processing underwent proteolysis in *B. subtilis* to yield intermediate forms. We have not noticed this before with a different *spoIVBSA378* mutant which was placed at the *spoIVB* locus (36). We believe that one possible explanation is that even though an active site residue is mutated, the protease can still retain residual proteolytic activity (20). Despite mutation of all three members of the catalytic His-Asp-Ser triad of subtilisin, enzymatic activity is still approximately  $10^3$  to  $10^4$  times the noncatalyzed rate (5). Our *in vivo* work shows that changes at His236, Asp363, and Ser378 do appear to allow limited self-cleavage of SpoIVB to forms of approximately 46, 45, and 44 kDa. We had previously predicted that



these might represent active forms but we must now question this model. It is possible, though, that the 44- to 46-kDa species observed in these mutants are actually inactive forms brought about by incorrect cleavage or by secondary proteolysis. Alternatively, residual enzyme activity is sufficient to permit self-cleavage but at levels too low to permit signaling. Our work does show clearly, though, that all nonsignaling mutants show delayed cleavage of the full-length form of SpoIVB, and we wonder whether signaling can occur only during a precise window of time concurrent with release of SpoIVB from the inner forespore membrane by self-cleavage. This latter event would occur following the first cut, and for signaling this is presumably then the most important event, enabling release of SpoIVB. In the nonsignaling mutants, though, we reason that self-processing is substantially reduced, leading to a delayed appearance of intermediate species, at which time the SpoIVFB processing complex is no longer responsive (or competent) to cleave pro- $\sigma^K$ .

The results of mutation at residues Asn290 and His394 are more difficult to interpret. Our work suggests that proteolysis of these mutants was less potent, leading to delayed signaling. Possible explanations include roles for these residues in ground state substrate binding or stabilization of the reaction transition state by forming an oxyanion hole reminiscent of Asn155 in subtilisin. Mutation of this sidechain leads to a 200- to 300-fold reduction in turnover number of this serine peptidase (4). A similar role for Asn290 might explain a delay in signaling.

We are presently attempting to determine the crystal structure of SpoIVB, which will enable us to test our prediction that Asp363 is suitably placed to comprise the third member of a catalytic triad and to assess the importance of residues Asn290 and His394 in SpoIVB function. We will also explore the role of the PDZ domain in relation to the peptidase activity. A survey of bacterial proteins with PDZ domains suggests that of 187 non-SpoIVB bacterial PDZ-containing proteins, remarkably only 9 are predicted not to contain transit peptides or transmembrane segments. More surprising is that only 28 are not associated with a protease activity, i.e., 85% of all known PDZ-containing bacterial proteins are also proteases (Fig. 5), indicating that they have evolved a specialized role in association with peptidase activity due to their ability to traverse a membrane for (i) localization and (ii) substrate specificity, and thus are ideal for the signaling function of SpoIVB.

#### ACKNOWLEDGMENTS

We would like to thank Tony Wilkinson and Phil Wakeley for their help and advice.

This work was supported by a grant from the Biotechnology and Biological Sciences Research Council (BBSRC) to S.M.C. J.A.B. is supported by the BBSRC-funded Structural Biology Centre at York.

#### REFERENCES

- Barrett, A. J., D. Rawlings, and J. F. Woessner (ed.). 1998. Handbook of proteolytic enzymes. Academic Press, San Diego, Calif.
- Barton, G. L. 1993. ALSCRIPT: a tool to format multiple sequence alignments. *Protein Eng.* **6**:37–40.
- Beebe, K. D., J. Shin, J. Peng, C. Chaudhury, J. Khera, and D. Pei. 2000. Substrate recognition through a PDZ domain in tail-specific protease. *Biochemistry* **39**:3149–3155.
- Bryan, P., M. W. Pantoliano, S. G. Quill, H.-Y. Hsiao, and T. Poulos. 1986. Site-directed mutagenesis and the role of the oxyanion hole in subtilisin. *Proc. Natl. Acad. Sci. USA* **83**:3743–3745.
- Carter, P. H., and J. A. Wells. 1988. Dissecting the catalytic triad of a serine peptidase. *Nature* **332**:564–568.
- Craik, C. S., S. Rocznai, C. Largman, and W. J. Rutter. 1987. The catalytic role of the active site aspartic acid in serine proteases. *Science* **237**:909–913.
- Cutting, S., A. Driks, R. Schmidt, B. Kunkel, and R. Losick. 1991. Forespore-specific transcription of a gene in the signal transduction pathway that governs pro- $\sigma^K$  processing in *Bacillus subtilis*. *Genes Dev.* **5**:456–466.
- Cutting, S., V. Oke, A. Driks, R. Losick, S. Lu, and L. Kroos. 1990. A forespore checkpoint for mother cell gene expression during development in *B. subtilis*. *Cell* **62**:239–250.
- Cutting, S., S. Panzer, and R. Losick. 1989. Regulatory studies on the promoter for a gene governing synthesis and assembly of the spore coat in *Bacillus subtilis*. *J. Mol. Biol.* **207**:393–404.
- Cutting, S., S. Roels, and R. Losick. 1991. Sporulation operon *spoIVF* and the characterization of mutations that uncouple mother-cell from forespore gene expression in *Bacillus subtilis*. *J. Mol. Biol.* **221**:1237–1256.
- Cutting, S. M., and P. B. Vander-Horn. 1990. Genetic analysis, p. 27–74. In C. R. Harwood and S. M. Cutting (ed.), *Molecular biological methods for Bacillus*. John Wiley & Sons Ltd., Chichester, United Kingdom.
- Green, D. H., and S. M. Cutting. 2000. Membrane topology of the *Bacillus subtilis* pro- $\sigma^K$  processing complex. *J. Bacteriol.* **182**:278–285.
- Hakansson, K., A. H.-J. Wang, and C. G. Miller. 2000. The structure of aspartyl dipeptidase reveals a unique fold with a Ser-His-Glu catalytic triad. *Proc. Natl. Acad. Sci. USA* **97**:14097–14102.
- Ho, N. T., J. A. Brannigan, and S. M. Cutting. 2001. The PDZ domain of the SpoIVB serine peptidase facilitates multiple interactions. *J. Bacteriol.* **183**:4364–4373.
- Kingma, R. L., M. Fragiathaki, H. J. Snijder, B. W. Dijkstra, H. M. Verheij, N. Dekker, and M. R. Egmond. 2000. Unusual catalytic triad of *Escherichia coli* outer membrane phospholipase A. *Biochemistry* **39**:10017–10022.
- Nicholson, W. L., and P. Setlow. 1990. Sporulation, germination and outgrowth, p. 391–450. In C. R. Harwood and S. M. Cutting (ed.), *Molecular biological methods for Bacillus*. John Wiley & Sons Ltd., Chichester, United Kingdom.
- Oke, V., M. Schepetov, and S. Cutting. 1997. SpoIVB has two distinct functions during spore formation in *Bacillus subtilis*. *Mol. Microbiol.* **23**:223–230.
- Pallen, M. J., and C. P. Ponting. 1997. PDZ domains in bacterial proteins. *Mol. Microbiol.* **26**:411–415.
- Pallen, M. J., and B. W. Wren. 1997. The HtrA family of serine proteases. *Mol. Microbiol.* **26**:209–221.
- Peracchi, A. 2001. Enzyme catalysis: removing chemically “essential” residues by site-directed mutagenesis. *Trends Biochem. Sci.* **26**:497–503.
- Ponting, C. P. 1997. Evidence for PDZ domains in bacteria, yeast, and plants. *Protein Sci.* **6**:464–468.
- Ponting, C. P., C. Philips, K. E. Davies, and D. J. Blake. 1997. PDZ domains: targeting signalling molecules to sub-membraneous sites. *BioEssays* **19**:469–479.
- Rawlings, N. D., and A. J. Barrett. 1994. Families of serine peptidases. *Methods Enzymol.* **244**:19–61.
- Rawlings, N. D., and A. J. Barrett. 2000. MEROPS: the peptidase database. *Nucleic Acids Res.* **28**:323–325.
- Resnekov, O. 1999. Role of the sporulation protein BofA in regulating activation of the *Bacillus subtilis* developmental transcription factor  $\sigma^K$ . *J. Bacteriol.* **181**:5384–5388.
- Resnekov, O., and R. Losick. 1998. Negative regulation of the proteolytic activation of a transcription factor in *Bacillus subtilis*. *Proc. Natl. Acad. Sci. USA* **95**:3162–3167.
- Ricca, E., S. Cutting, and R. Losick. 1992. Characterization of *bofA*, a gene involved in intercompartmental regulation of pro- $\sigma^K$  processing during sporulation in *Bacillus subtilis*. *J. Bacteriol.* **174**:3177–3184.
- Rudner, D. Z., P. Fawcett, and R. Losick. 1999. A family of membrane-embedded metalloproteases involved in regulated proteolysis of membrane-associated transcription factors. *Proc. Natl. Acad. Sci. USA* **96**:14765–14770.
- Sambrook, J., E. F. Fritsch, and T. Maniatis. 1989. *Molecular cloning: a laboratory manual*, 2nd ed. Cold Spring Harbor Laboratory Press, Cold Spring Harbor, N.Y.
- Sandman, K., L. Kroos, S. Cutting, P. Youngman, and R. Losick. 1988. Identification of the promoter for a spore coat protein gene in *Bacillus subtilis* and studies on the regulation of its induction at a late stage of sporulation. *J. Mol. Biol.* **200**:461–473.
- Schultz, J., R. R. Copley, T. Doerks, C. P. Ponting, and P. Bork. 2000. SMART: a web-based tool for the study of genetically mobile domains. *Nucleic Acids Res.* **28**:231–234.
- Thompson, J. D., D. G. Higgins, and T. J. Gibson. 1994. CLUSTAL W: improving the sensitivity of progressive multiple sequence alignment through sequence weighting, position-specific gap penalties and weight matrix choice. *Nucleic Acids Res.* **22**:4673–4680.
- Tong, L., C. Qian, M.-J. Massariol, P. R. Bonneau, M. G. Cordingley, and L. Lagace. 1996. A new serine-protease fold revealed by the crystal structure of human cytomegalovirus protease. *Nature* **383**:272–275.
- Varcamonti, M., R. Marasco, M. De Felice, and M. Sacco. 1997. Membrane topology analysis of the *Bacillus subtilis* BofA protein involved in pro- $\sigma^K$



- processing. *Microbiology* **143**:1053–1058.
35. **Vernet, T., D. C. Tessier, J. Chatellier, C. Plouffe, T. S. Lee, D. Y. Thomas, A. C. Storer, and R. Menard.** 1995. Structural and functional roles of asparagine 175 in the cysteine protease papain. *J. Biol. Chem.* **270**:16645–16652.
  36. **Wakeley, P., R. Dorazi, N. T. Hoa, J. R. Bowyer, and S. M. Cutting.** 2000. Proteolysis of SpoIVB is a critical determinant in signalling of pro- $\sigma^K$  processing in *Bacillus subtilis*. *Mol. Microbiol.* **36**:1336–1348.
  37. **Wlodawer, A., M. Li, Z. Dauter, A. Gustchina, K. Uchida, H. Oyama, B. M. Dunn, and K. Oda.** 2001. Carboxyl proteinase from *Pseudomonas* defines a novel family of subtilisin-like enzymes. *Nat. Struct. Biol.* **8**:442–446.
  38. **Youngman, P., J. Perkins, and R. Losick.** 1984. Construction of a cloning site near one end of Tn917 into which foreign DNA may be inserted without affecting transposition in *Bacillus subtilis* or expression of the transposon-borne *erm* gene. *Plasmid* **12**:1–9.